Supplemental Document

Optics Letters

Shaping convex edges in borosilicate glass by single pass perforation with an Airy beam: supplement

DAVID SOHR,[1,2,*] JENS ULRICH THOMAS,[2] AND STEFAN SKUPIN[1]

[1] *Institut Lumière Matière, UMR 5306 Université Lyon 1-CNRS, Université de Lyon, Villeurbanne 69622, France*
[2] *SCHOTT AG, Hattenbergstrasse 10, Mainz 55122, Germany*
[*] *Corresponding author: david.sohr@univ-lyon1.fr*

Supplement DOI: https://doi.org/10.6084/m9.figshare.14498013

Parent Article DOI: https://doi.org/10.1364/OL.423788

Shaping convex edges in borosilicate glass by single pass perforation with an Airy beam: supplemental document

1. FURTHER NUMERICAL RESULTS

Here we show and discuss further results of the nonlinear simulations, namely the volume density of the deposited energy ρ_V, as shown in Fig. 2d of the main text and in Fig. S2, and its integral across the transversal xy-plane, giving the line energy density ρ_L along the propagation axis z as shown in Fig. S1. The values of the line energy density ρ_L increase with increasing pulse energy and decreasing pulse duration respectively, as does the asymmetry of its distribution. The preferential energy deposition in front of the linear focus is particularly prominent for the highest pulse power considered here, see Fig. S1, 1 ps, 352 µJ. Note however, that at the position of the peak of ρ_L in this case no volume modification can be seen in light microscopy cross section, as shown in Fig. 2c) of the main text. This is because the corresponding volume energy density ρ_V is low and broadly distributed (no steep gradients), cf. Fig. S2. Only further along the propagation path a narrow central absorption peak is formed. It is remarkable that the peak values of ρ_V throughout the entire propagation in this case remain below those of the lowest pulse energy case considered for $t_p = 10\,\text{ps}$. Ignition of a plasma in the side lobes of the Airy pattern earlier in the propagation is much more pronounced for the shorter and thus more intense 1 ps pulses. This causes absorption and deflection of significant parts of the pulse and diminishes the energy flow to the main Airy lobe. A significant energy deposition in the side lobes in front of the linear focus and a more confined energy density distribution close to the main lobe trajectory behind it are observed for all but the lowest pulse power (10 ps, 68 µJ). This agrees well with the observed morphology of volume modifications in glass.

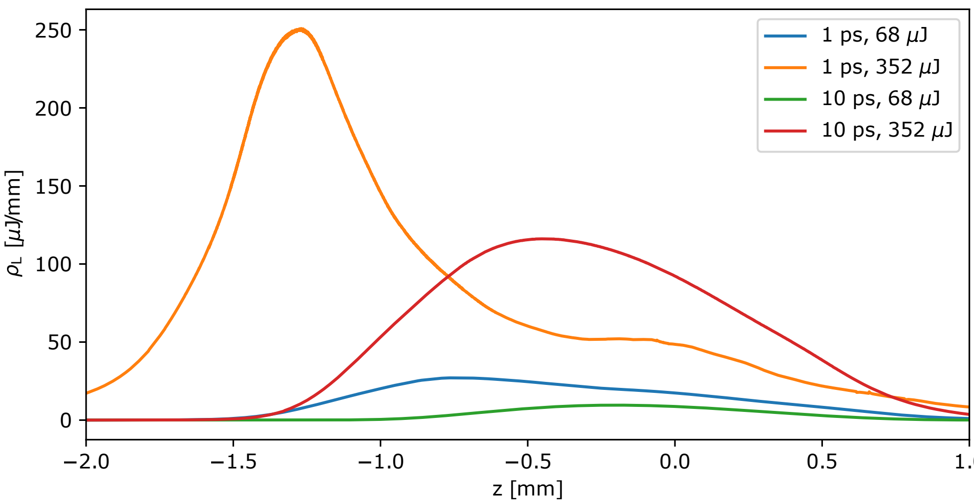

Fig. S1. Line density of deposited energy ρ_L for the two pulse durations and the two pulse energies shown in Fig. 2d of the main text. Note the shift of the distribution towards the laser source with respect to the linear focus position at $z = 0$ with increasing pulse power.

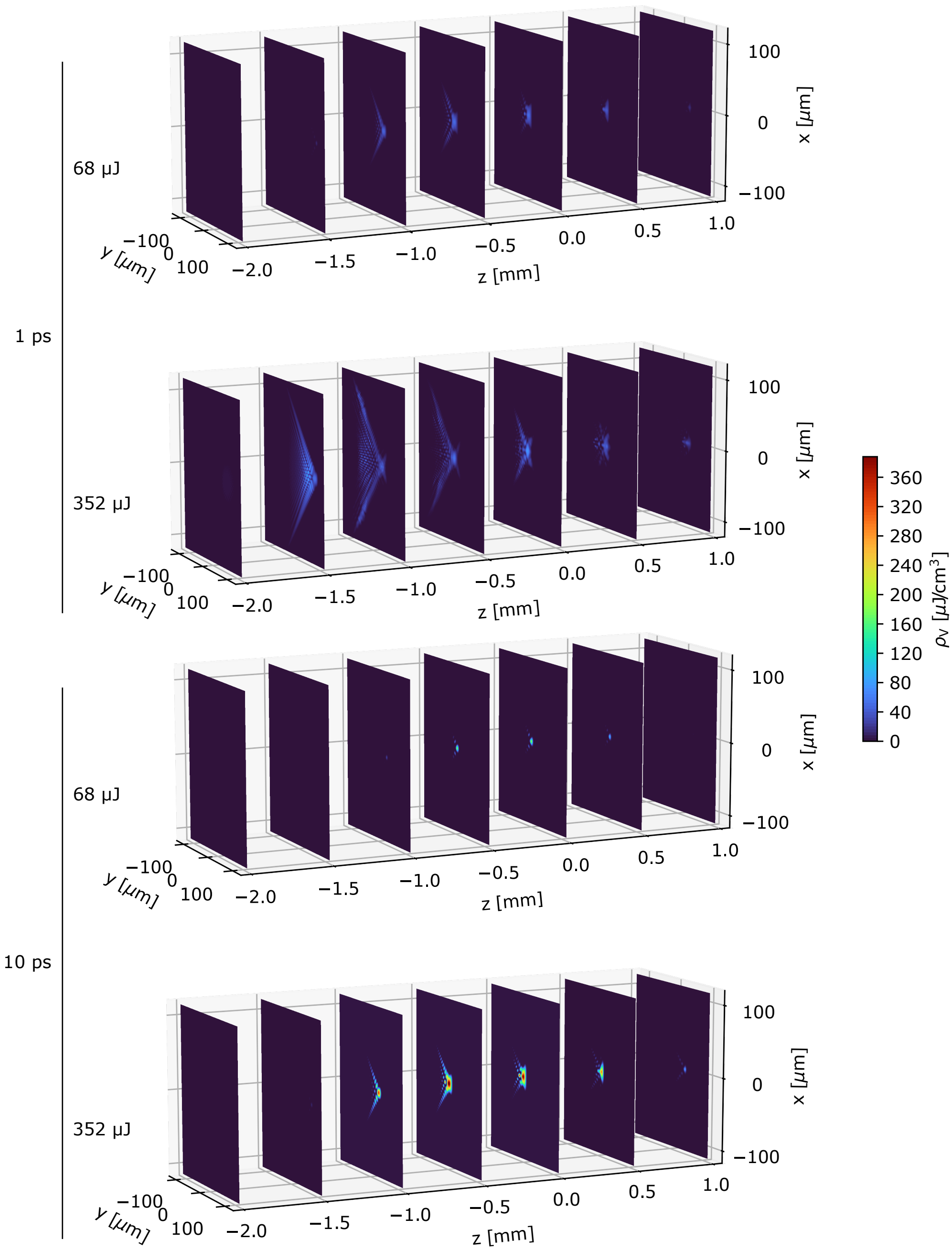

Fig. S2. Transversal sections of the volume density of deposited energy ρ_V for pulsed Airy beams with the same pulse configurations as in Fig. S1. The sections at the linear focus position $z = 0$ correspond to those shown in Fig. 2d of the main text.

2. DETAILS ON THE SEPARATION PROCESS

As mentioned in the main text, we could separate 525 µm thick glass sheets both by cleaving and by etching after laser processing with an Airy beam with $f = 10$ mm, $t_p = 5$ fs, 2 pulse burst and a pitch of 10 µm each.

Mechanical cleaving For best results the mechanical cleaving required a focus position beneath the center of the sheet ($\Delta z = 250$ µm) and a burst energy E_{burst} of 428 µJ, i.e. a slightly more asymmetric focus position and nearly twice the burst energy compared to etching. While the crack in some parts follows the laser perforations throughout the full thickness of the material, the concoidal fracture that occurs frequently along the intended cutting surface can clearly be seen in Fig. S3. Neither the concave nor the convex side of the cut have a well defined profile after mechanical cleaving.

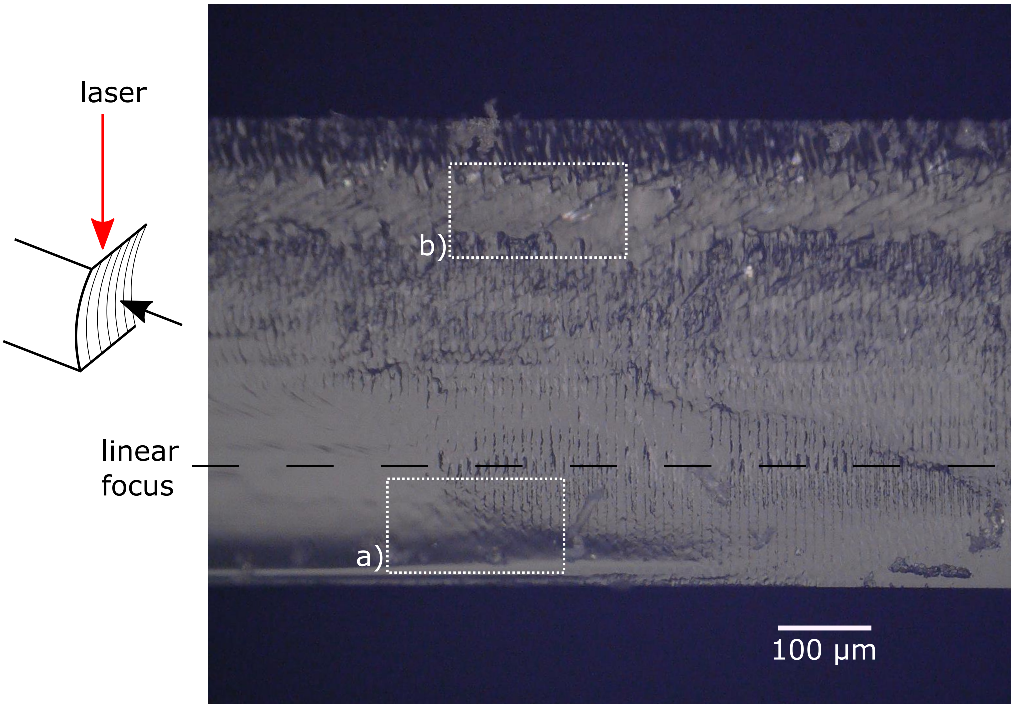

Fig. S3. Side view onto concave side of a glass sheet cleaved mechanically after laser perforation with $E_{burst} = 428$ µJ from the top as shown on the left. Note that while the laser modifications penetrate the whole thickness of the sheet, large parts are fractured concoidally, leaving glass superimposed on the surface of modifications (a). This means that neither the concave nor the convex side of the cut have a well defined profile. A zone towards the surface shows hardly any laser modification (b). We interprete this as the shadow of the plasma ignited at the surface during the laser process.

Etching As shown in Fig. 4 of the main text separation by etching (50 µm etching depth in the pristine material) with potassium hydroxide yields a smooth convex edge of the sample. Using the increased etching rate in laser modified zones of glass is an established technique [1, 2] and applied in several industrial processes [3–6]. The selectivity S, that is the ratio between the etching rates of modified and pristine material respectively, strongly depends on the parameters of the etching process, but also on the material itself and the extent of laser damage adjusted by the parameters of the laser process [7]. For isotropic etching with a finite selectivity a laser modification which is perpendicular to the substrate surface will result in a corner with an angle larger than 90° by an angle θ_t which is called taper. By comparing the profile of the edge with the calculated trajectory of the focal intensity, we estimate the contribution of the etching process to the top angle in our etched sample to be about 8°. Approximating the relationship between selectivity and taper as $S \approx \cot \theta_t$ (see Fig. S4), we get a value of about 7 for the selectivity, which agrees well with the low values previously published for borosilicate glass [5].

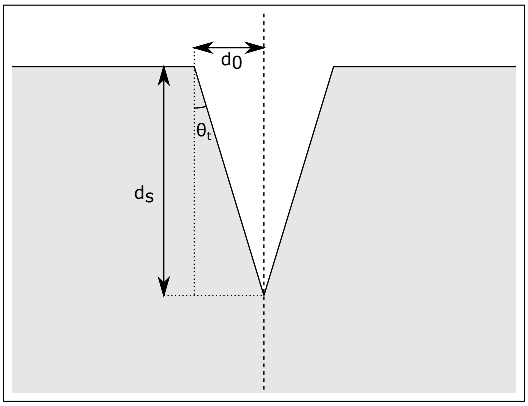

Fig. S4. Sketch demonstrating the relationship between taper θ_t and etching depths in unit time d_0 in pristine and d_s in modified material respectively for an infinitely thin laser modification (dashed line) and $d_s \gg d_0$.

REFERENCES

1. J. Gottmann, "Microcutting and hollow 3d microstructures in glasses by in-volume selective laser-induced etching (isle)," J. Laser Micro/Nanoengineering **8**, 15–18 (2013).
2. D. Flamm, D. Grossmann, M. Kaiser, J. Kleiner, M. Kumkar, K. Bergner, and S. Nolte, "Tuning the energy deposition of ultrashort pulses inside transparent materials for laser cutting applications," Proc. LiM **253** (2015).
3. A. Ortner, A. Roters, F.-T. Lentes, L. Parthier, M. Heiß-Choquet, U. Peuchert, F. Wagner, F. Resch, L. Brückbauer, M. Jotz *et al.*, "Structured plate-like glass element and process for the production thereof," (2018). US Patent App. 15/882,187.
4. Y. Jin and M. E. Wilhelm, "Glass-based substrate with vias and process of forming the same," (2017). US Patent App. 15/286,803.
5. "SLE-Prozess - LightFab," https://lightfab.de/files/Downloads/LightFab_DS_SLE.pdf.
6. "Micromachining of Glass by Laser Induced Deep Etching (LIDE) - LPKF Vitrion® 5000," https://jp.lpkf.com/_mediafiles/3763-lpkf-vitrion-5000-en.pdf.
7. Martin Hermans, Jens Gottmann, and Frank Riedel, "Selective, laser-induced etching of fused silica at high scan-speeds using KOH," J. Laser Micro / Nanoeng. **9** (2014).